

# Sinusoidal wavelength-scanning interferometers

Osami Sasaki, Kenichiro Tsuji, Shouichi Sato, Tomokazu Kuwahara,  
and Takamasa Suzuki

Niigata University, Faculty of Engineering  
8050 Ikarashi 2, Niigata-shi 950-21, Japan  
Fax 81-25-263-3174 E-mail osami@eng.niigata-u.ac.jp

## ABSTRACT

In sinusoidal phase-modulating interferometry an optical path length (OPD) larger than a wavelength is measured by detecting sinusoidal phase-modulation amplitude of the interference signal. This interference signal is produced by scanning sinusoidally wavelength of a light source. If the measurement accuracy in OPD is higher than half of the central wavelength, this measured value is combined with a fractional value of the OPD which is obtained from the conventional phase of the interference signal. The measurement accuracy in OPD is higher as the scanning width of wavelength is larger. We propose two different methods to create a light source with a large scanning width of wavelength by using superluminescent laser diode and external-cavity tunable laser diode. Experimental results clearly show that sinusoidal wavelength-scanning interferometers using these light sources measure an OPD over a few tens of microns with a high accuracy of a few nm.

## 1. INTRODUCTION

Single-wavelength interferometers are limited to measurements of smooth and continuous surfaces on which a change of the optical path difference (OPD) between two measuring points is smaller than a half wavelength. A method to overcome this limitation is to use a number of wavelengths whose phases of an interference signal determine an OPD longer than a wavelength. This method leads to two-wavelength interferometers<sup>1-6</sup>, wavelength-scanning interferometers<sup>6-10</sup>, and dispersive white-light interferometers<sup>11-16</sup> or white-light channelled spectrum interferometers. In two-wavelength interferometers the two wavelengths offer a synthetic wavelength longer than each of the two wavelengths. Combination between an OPD measured with the synthetic wavelength and an OPD measured with a single wavelength requests a very high stability of the two wavelengths. Wavelength-scanning interferometers detect how a phase of interference signal changes in time domain when the wavelength of a source is scanned with time. Measurement accuracy in OPD is higher as the scanning width of wavelength is larger. Dispersive white-light interferometers observe a phase distribution of interferogram for wavelength in space domain with help of a diffraction grating. Another method to determine an OPD longer than a wavelength is to use the property that visibility of interferogram generated by white-light is maximum when the OPD is zero. White-light interferometers<sup>17-19</sup> look for positions of OPD=0 on object surface by giving mechanical displacements to the reference surface.

In this paper sinusoidal wavelength-scanning (SWS) interferometers are described in which sinusoidal phase-modulating interferometry<sup>21</sup> is used. A SWS light source produces a sinusoidally phase-modulated interference signal, and its phase-modulation amplitude is proportional to OPD and the scanning width of wavelength. In SWS interferometers an OPD longer than a wavelength is measured from detection of the phase-modulation amplitude. At a same time a fractional value of the OPD is measured with a high accuracy of a few nm from detection of the conventional phase of interference signal. If the measurement accuracy in an OPD longer than a wavelength is higher than a half wavelength, these two measured values can be combined. This combination enables us to measure an OPD longer than a wavelength with a high accuracy of a few nm.

Although widely used laser diodes whose wavelength is changed by its injection current is a SWS light source, the continuous scanning width is not large enough to measure an OPD with an accuracy higher than a half wavelength. We propose SWS interferometers using two different light sources with a large scanning width of wavelength. A superluminescent laser diode (SLD) and an external-cavity tunable laser diode (TLD)<sup>21</sup> are used for creating the SWS light sources. In a SWS light source using SLD, its continuous spectrum obtained with a diffraction grating is filtered by a sinusoidally moving slit. In a SWS light source using an external-cavity TLD a mirror is rotated sinusoidally which reflects a beam incident to a diffraction grating. Since sinusoidal movements of a slit or a mirror are easily made compared to other movements, SWS can be exactly achieved. Interferometers using these light sources are called SWS-SLD interferometer and SWS-TLD interferometer, respectively. The two SWS interferometers are constructed, and some fundamental experimental results show clearly characteristics of the interferometers.

## 2. SWS INTERFEROMETER

Figure 1 shows a Michelson interferometer using a SWS light source whose wavelength is sinusoidally scanned as

$$\lambda(t) = \lambda_0 + \Delta\lambda(t) = \lambda_0 + b \cos(\omega_b t). \quad (1)$$

This interferometer is termed SWS interferometer. Collimated output beam from a SWS light source is divided into

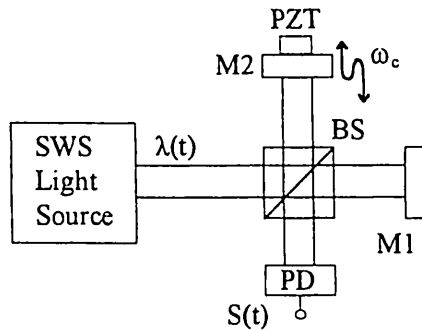


Fig.1 SWS interferometer.

two beams. One of them is reflected by mirror M1 which is used as an object. The other one is reflected by mirror M2 which is sinusoidally vibrated by a piezoelectric transducer (PZT) with angular frequency  $\omega_c$  to adapt double sinusoidal phase-modulating interferometry<sup>8</sup>. Denoting an OPD by  $L$ , a phase of an interference signal is approximated as

$$\Psi(t) = 2\pi L/\lambda(t) = -2\pi[\Delta\lambda(t)/\lambda_0^2]L + (2\pi/\lambda_0)L, \quad (2)$$

in the condition of  $b \ll \lambda_0$ . Considering the sinusoidal phase modulation by mirror M2, intensity change  $M(t)$  of the output beam from a SWS light source, and visibility  $V$ , an interference signal detected with a photo diode (PD) is given by

$$S(t) = M(t) + M(t)V \cos(Z_c \cos \omega_c t + Z_b \cos \omega_b t + \alpha), \quad (3)$$

where,  $Z_c = 4\pi a/\lambda_0$ , and

$$Z_b = (2\pi b/\lambda_0^2)L, \quad (4)$$

$$\alpha = -(2\pi/\lambda_0)L. \quad (5)$$

By processing signal  $S(t)$  using Fourier-transform as described in Ref.8, we obtain

$$\phi(t) = Z_b \cos \omega_b t + \alpha. \quad (6)$$

The carrier signal of  $Z_c \cos \omega_c t$  plays an important role in calculating an value of  $\phi(t)$  with a high accuracy. Fourier-transform of  $\phi(t)$  provides us values of  $Z_b$  and  $\alpha$ .

The value of proportional constant  $2\pi b/\lambda_0^2$  is determined by measuring  $Z_b$  for different values of OPD. After that, measurement of  $Z_b$  provides a value of OPD which is denoted by  $L_z$ . We also obtain a fractional value of OPD from the value of  $\alpha$  which is denoted by  $L_\alpha$ . Since a value of  $\alpha$  is expressed in the range from  $-\pi$  to  $\pi$ , a value of  $L_\alpha$

is in the range from  $-\lambda_0/2$  to  $\lambda_0/2$  and its measurement accuracy is a few nm. OPD  $L$  that represents the absolute distance is given by

$$L = m\lambda_0 + L_\alpha, \quad (7)$$

and integer  $m$  can be obtained by rounding off the following number to an integer if measurement accuracy of  $L_z$  is higher than  $\lambda_0/2$ :

$$m_c = (L_z - L_\alpha)/\lambda_0, \quad (8)$$

This measurement accuracy in  $L_z$  is achieved for a large value of  $b$ . When there are random errors in detection of  $Z_b$ , averaging a lot of measured values of  $m_c$  is effective for determination of  $m$ . In SWS interferometer the combination of two measured values of  $L_z$  and  $L_\alpha$  results in an exact OPD measurement over a few tens of microns with a high accuracy of a few nm.

### 3. SWS-SLD INTERFEROMETER

#### A. CONFIGURATION

Figure 2 shows a SWS interferometer using a SLD. Output beam from the SLD is collimated with lens L1 and incident on diffraction grating G1. The first-order reflection from the grating is Fourier transformed with lens L2 to perform a grating spectroscope. A continuous spectrum of the SLD shown in Fig.3 is displayed on a focal plane of lens L2 and L3. A central wavelength of the spectrum is  $\lambda_0$ . Slit SL put on the focal plane transmits a portion of the spectrum. The slit is connected with a magnetic coil of a speaker and vibrated sinusoidally with an angular frequency of  $\omega_b$ . The central wavelength of the light passing through the slit is sinusoidally scanned as shown in Fig.3, and it is expressed by Eq.(1). The light coming out of the slit is Fourier transformed with lens L3 and incident on grating G2 so that the first order reflection from the grating produces a collimated beam whose propagating direction is constant for all of wavelengths contained in the spectrum of the SLD. The collimated beam becomes a SWS light source for an interferometer.

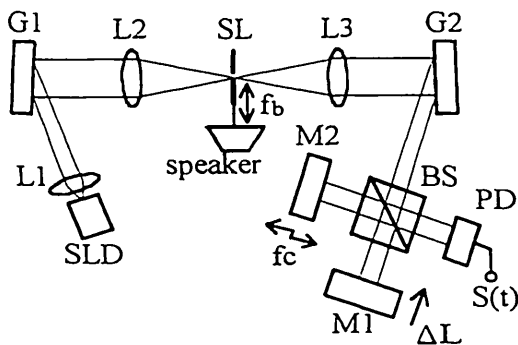


Fig.2 SWS interferometer using a SLD.

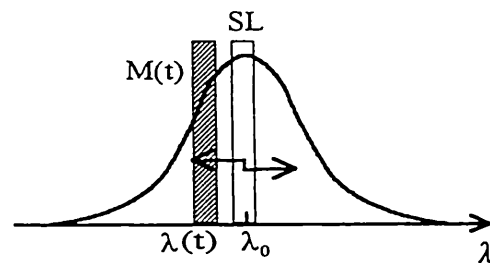


Fig.3 Continuous spectrum of a SLD and its filtering.

A SWS-SLD interferometer was constructed. Central wavelength  $\lambda_0$  and spectral bandwidth of the SLD were 789.3 nm and 20 nm, respectively. An 1200-line/mm blazed grating was used for G1 and G2. The angular frequencies of  $\omega_b/2\pi$  and  $\omega_s/2\pi$  were 30 Hz and 480 Hz, respectively.

#### B. EXPERIMENTAL RESULTS

Figures 4 shows the vibration of the slit and an interference signal detected when mirror M2 was at rest, that is,  $Z_c=0$ . Interference signal  $S(t)$  detected when mirror M2 was vibrating was sampled with an analog-to-digital converter to be processed in a micro-computer. The sampling frequency was  $8 \times (\omega_s/2\pi)$ . Phase  $\phi(t)$  and amplitude of its Fourier transform are shown in Fig.5. The value of  $Z_b$  was obtained from the amplitude of 30 Hz component, and it was  $2 \times 0.46$  rad

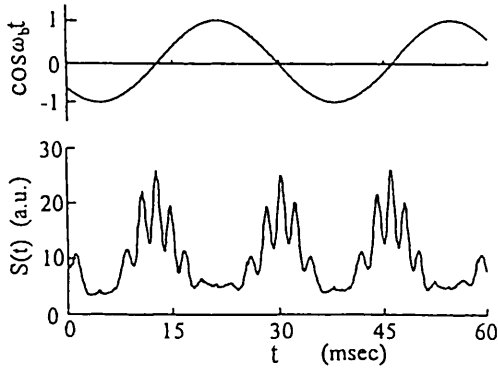


Fig.4 Vibration of the slit and an interference signal detected when mirror M2 was at rest.

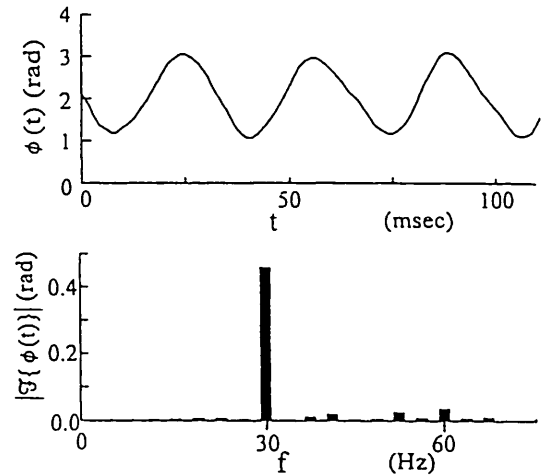


Fig.5 Phase  $\phi(t)$  and amplitude of its Fourier transform.

We gave a displacement to mirror M1 fixed on a stage by means of a micrometer to change the OPD by  $1.0 \mu\text{m}$ . Figure 6 shows values of  $Z_b$  measured for different values of change  $\Delta L$  in OPD. From these results we obtain a relationship between  $Z_b$  and  $L$ , which is  $Z_b = 0.0870 \times L (\mu\text{m})$ . The proportional constant leads to width  $2b$  of the wavelength-scanning of  $17.3 \text{ nm}$ . Figure 7 shows variation of  $Z_b$  with time when  $\Delta L = 7 \mu\text{m}$ . Values of  $Z_b$  obtained from ten set data detected at intervals of 10 seconds are distributed in a vertical direction at a fixed time in horizontal axis. This detection was repeated at intervals of 1 minute. It is concluded from these results that OPD can be measured from  $Z_b$  with an accuracy of  $0.26 \mu\text{m}$ . Since this accuracy is higher than half of wavelength  $\lambda_0$ , the combination of  $L_z$  and  $L_\alpha$  is possible.

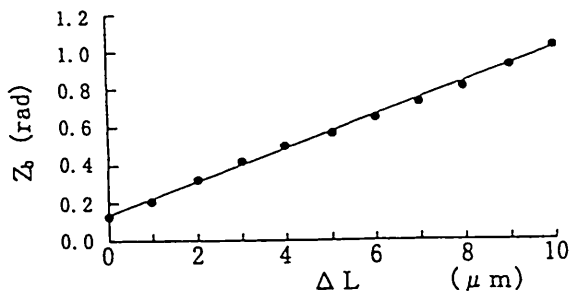


Fig.6 Values of  $Z_b$  measured for different values of change  $\Delta L$  in OPD.

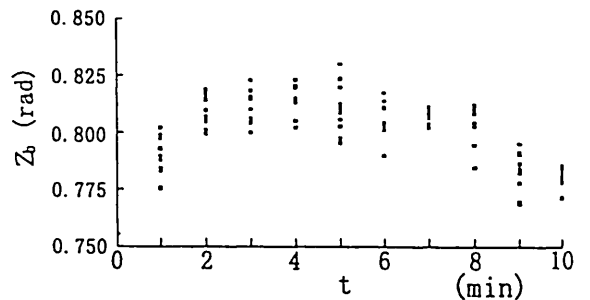


Fig.7 Variation of  $Z_b$  with time when  $\Delta L = 7 \mu\text{m}$ .

We obtained ten set values of  $L_z$  and  $L_\alpha$  for one value of change  $\Delta L$ , and calculated number  $m_c$ . We selected three set values of  $L_z$  and  $L_\alpha$  which correspond to maximum, nearly mean, and minimum values of  $m_c$ , respectively. The results are shown in Table 1 for two different values of  $\Delta L$ . Since difference between a value of  $m_c$  and an integer of its round number is within 0.3, an exact OPD can be obtained after determination of integer  $m$ . Variations of  $L_\alpha$  is caused by external disturbances to the experimental setup. Table 2 shows measured values for other values of  $\Delta L$  increased at intervals of  $1.0 \mu\text{m}$ , and the corresponding actual increase in  $L$ .

**Table 1. Measured Values and  $m_c$**

| $\Delta L(\mu\text{m})$ | Data No. | $L_z(\text{nm})$ | $L_\alpha(\text{nm})$ | $m_c$ | $L(\text{nm})$ |
|-------------------------|----------|------------------|-----------------------|-------|----------------|
| 0                       | 1        | 1338             | -190                  | 1.9   | 1388           |
| 0                       | 2        | 1403             | -193                  | 2.0   | 1385           |
| 0                       | 3        | 1589             | -189                  | 2.2   | 1389           |
| 5                       | 1        | 6418             | 196                   | 7.9   | 6510           |
| 5                       | 2        | 6541             | 190                   | 8.0   | 6505           |
| 5                       | 3        | 6656             | 195                   | 8.2   | 6509           |

**Table 2. Measured Values**

| $\Delta L(\mu\text{m})$ | $L_z(\text{nm})$ | $L_\alpha(\text{nm})$ | $m$ | $L(\text{nm})$ | Increase in $L(\text{nm})$ |
|-------------------------|------------------|-----------------------|-----|----------------|----------------------------|
| 1                       | 2565             | 101                   | 3   | 2469           | 1083                       |
| 2                       | 3692             | 365                   | 4   | 3522           | 1053                       |
| 3                       | 4674             | -145                  | 6   | 4590           | 1068                       |
| 4                       | 5659             | -113                  | 7   | 5412           | 822                        |

#### 4. SWS-TLD INTERFEROMETER A. CONFIGURATION

Figure 8 shows a SWS interferometer using a TLD. Output beam from a LD is collimated with lens L and incident on diffraction grating G. The first-order reflection from the grating is reflected back into the LD with mirror M. The zero-order reflection from the grating is the output beam of the SWS-TLD. One end of the laser cavity is the rear facet of the LD, and the other end is mirror M. The wavelength is scanned by rotating mirror M sinusoidally with an angular frequency  $\omega_b$ .

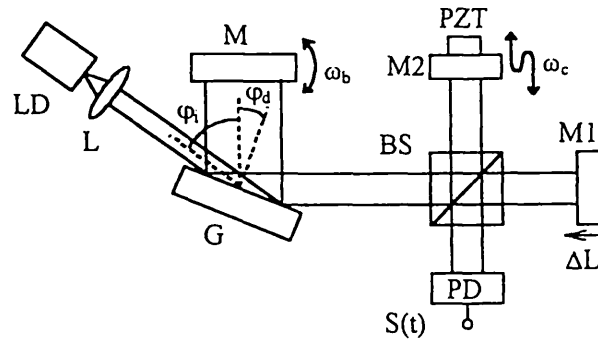


**Fig.8 SWS interferometer using a TLD.**

The diffraction angle of the first-order is expressed as

$$\varphi_d(t) = \varphi_{d0} + \Delta\varphi_d(t) = \varphi_{d0} + a \cos\omega_b t, \quad (9)$$

where  $\varphi_{d0}$  is an initial diffraction angle, and  $a$  is amplitude of the vibration angle of mirror M.

Substituting Eq.(9) to the grating equation

$$\lambda(t) = d [\sin\varphi_i - \sin\varphi_d(t)] = \lambda_0 + \Delta\lambda(t), \quad (10)$$

and using approximations of  $\cos\Delta\varphi_d(t) \approx 1$  and  $\sin\Delta\varphi_d(t) \approx \Delta\varphi_d(t)$ , we obtain

$$\Delta\lambda(t) = da \cos\varphi_{d0} \cos\omega_b t, \quad (11)$$

where  $d$  is the grating space.

A SWS-TLD interferometer was constructed. We used a LD whose central wavelength  $\lambda_0$  and output power were 783.3 nm and 50 mW, respectively. A 1200-line/mm holographic grating was used with angles  $\varphi_i$  of 75° and

$\varphi_{d0}$  of  $5^\circ$ . Mirror M was vibrated by a galvanometer optical scanner with amplitude  $a$  of 7.4 mrad. The angular frequencies of  $\omega_b/2\pi$  and  $\omega_c/2\pi$  were 40 Hz and 1280 Hz, respectively.

### B. EXPERIMENTAL RESULTS

Figure 9 shows an interference signal detected when mirror M2 was at rest, that is,  $Z_c=0$ . Intensity change  $M(t)$  of the SWS-TLD is much smaller than that of the SWS-SLD, but small amplitude changes with high frequency components appear in the interference signal. The sampling frequency for interference signal  $S(t)$  detected when mirror M2 was vibrating was  $8 \times (\omega_c/2\pi)$ . Phase  $\phi(t)$  and amplitude of its Fourier transform are shown in Fig. 10. The value of  $Z_b$  was obtained from the amplitude of 40 Hz component.

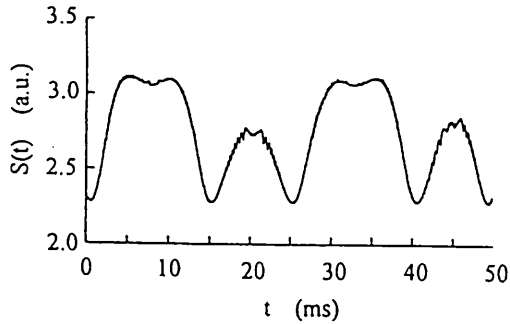


Fig.9 Interference signal detected when mirror M2 was at rest.

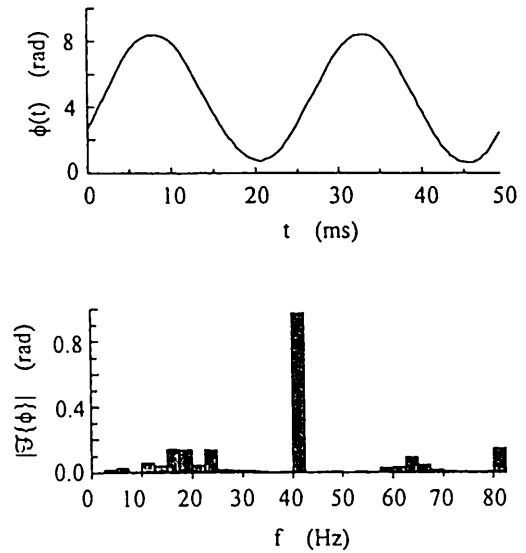


Fig.10 Phase  $\phi(t)$  and amplitude of its Fourier transform.

We gave a displacement to mirror M1 fixed on a stage by means of a micrometer to change the OPD by  $1.0 \mu\text{m}$ . Figure 11 shows values of  $Z_b$  measured for different values of change  $\Delta L$  in OPD. From these results we obtain a relationship of  $Z_b = 0.0315 \times L$  ( $\mu\text{m}$ ). The proportional constant means width  $2b$  of the wavelength-scanning of 6.15 nm. Figure 12 shows variation of  $Z_b$  with time. Values of  $Z_b$  obtained from five data detected at intervals of 30 seconds are distributed in a vertical direction for each value of change  $\Delta L$ . It is concluded from these results that OPD can be measured from  $Z_b$  with an accuracy of  $0.17 \mu\text{m}$ .

We obtained five set values of  $L_z$  and  $L_\alpha$  for one value of change  $\Delta L$ , and calculated number  $m_c$ . We selected three set values of  $L_z$  and  $L_\alpha$  which correspond to maximum, nearly mean, and minimum values of  $m_c$ , respectively. The results are shown in Table 3 for two different values of  $\Delta L$ . Difference between a value of  $m_c$  and an integer of its round number is within 0.4. Table 4 shows measured values for other values of  $\Delta L$  increased at intervals of  $1.0 \mu\text{m}$ , and the corresponding actual increase in  $L$ .

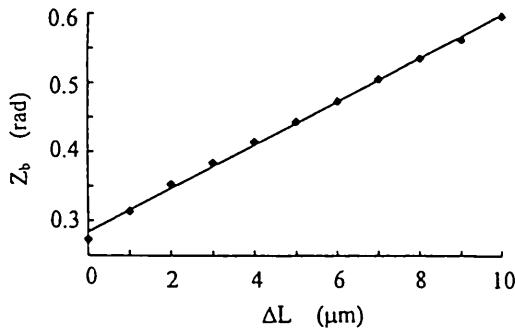


Fig.11 Values of  $Z_b$  measured for different values of change  $\Delta L$  in OPD.

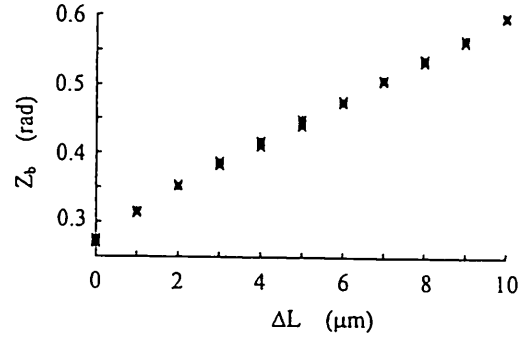


Fig.12 Variation of  $Z_b$  with time for different values of change  $\Delta L$  in OPD.

Table 3. Measured Values and  $m_c$

| $\Delta L(\mu\text{m})$ | Data No. | $L_z(\text{nm})$ | $L_\alpha(\text{nm})$ | $m_c$ | $L(\text{nm})$ |
|-------------------------|----------|------------------|-----------------------|-------|----------------|
| 0                       | 1        | 8533             | -54                   | 10.9  | 8562           |
| 0                       | 2        | 8669             | -42                   | 11.1  | 8573           |
| 0                       | 3        | 8771             | -78                   | 11.3  | 8537           |
| 5                       | 1        | 14054            | 321                   | 17.5  | 14420          |
| 5                       | 2        | 14133            | 291                   | 17.7  | 14390          |
| 5                       | 3        | 14279            | 268                   | 17.9  | 14367          |

Table 4. Measured Values

| $\Delta L(\mu\text{m})$ | $L_z(\text{nm})$ | $L_\alpha(\text{nm})$ | $m$ | $L(\text{nm})$ | Increase in $L(\text{nm})$ |
|-------------------------|------------------|-----------------------|-----|----------------|----------------------------|
| 1                       | 9946             | 164                   | 12  | 9563           | 1001                       |
| 2                       | 11158            | -40                   | 14  | 10926          | 1363                       |
| 3                       | 12184            | 289                   | 15  | 12038          | 1112                       |
| 4                       | 13222            | -39                   | 17  | 13277          | 1239                       |

## 5. CONCLUSION

We described how to measure an OPD larger than a wavelength with SWS interferometer. Since a large scanning width of wavelength was required for the measurement, we proposed two different SWS light sources using the SLD and the TLD, respectively. We constructed SWS interferometers using these light sources, and showed clearly their characteristics. Although there was a large intensity change in the light source of the SWS-SLD interferometer, a large scanning width of 17 nm was easily obtained. In the SWS-TLD interferometer an exact arrangement was required to obtain a large scanning width of 6 nm without any mode hop of wavelength. These interferometers could determine an integer  $m$  from the two measured values of  $L_z$  and  $L_\alpha$ , and measure an OPD with a high accuracy of a few nm in the range from a few microns to a few tens of microns.

## REFERENCES

1. C.Polhemus, "Two-wavelength interferometer," Appl. Opt. 12, 2071-2074 (1973).
2. K.Creath, "Step height measurement using two-wavelength phase-shifting interferometry," Appl. Opt. 26, 2810-2816 (1987).
3. P.de Groot and S.Kishner, "Synthetic wavelength stabilization for two-color laser-diode interferometry," Appl. Opt. 30, 4026-4033 (1991).

4. O.Sasaki, H.Sasazaki, and T.Suzuki, "Two-wavelength sinusoidal phase/modulating laser-diode interferometer insensitive to external disturbances," *Appl. Opt.* 30, 4040-4045 (1991).
5. V.Gusmeroli and M.Martinelli, "Two-wavelength interferometry by superluminescent source filtering," *Opt. Commun.* 94, 309-312 (1992).
6. R.Onodera and Y.Ishii, "Two-wavelength laser-diode interferometer with fractional fringe techniques," *Appl. Opt.* 34, 4740-4746 (1995).
7. H.kikuta, K.Iwata, and R.Nagata, "Distance measurement by the wavelength shift of laser diode light," *Appl. Opt.* 25, 2976-2980 (1986).
8. O.Sasaki, T.Yoshida, and T.Suzuki, "Double sinusoidal phase-modulating laser diode interferometer for distance measurement," *Appl. Opt.* 30, 3617-3621 (1991).
9. S.Kuwamura, I.Yamaguchi, "Wavelength scanning profilometry for real-time surface shape measurement," *Appl. Opt.* 36, 4473-4482 (1997).
10. F.Lexer, C.K.Hitzenberger, A.F.Fercher, and M.Kulhavy, "Wavelength-tuning interferometry of intraocular distances," *Appl. Opt.* 36, 6548-6553 (1997).
11. J.Schwider and L.Zhou, "Dispersive interferometric profilometer," *Opt. Lett.* 19, 995-997 (1994).
12. U.Schnell, E.Zimmermann, and R.Dandliker, "Absolute distance measurement with synchronously sampled white-light channelled spectrum interferometry," *Pure Appl. Opt.* 4, 643-651 (1995).
13. P.Sandoz, G.Tribillon, and H.Perrin, "High-resolution profilometry by using phase calculation algorithms for spectroscopic analysis of white-light interferograms," *J. of Mod. Opt.* 43, 701-708 (1996).
14. L.Rovati, U.Minoni, and F.Docchio, "Dispersive white-light combined with a frequency-modulated continuous-wave interferometer for high-resolution absolute measurements of distance," *Opt. Lett.* 22, 850-852 (1997).
15. T.Li, R.G.May, A.Wang, and R.O.Claus, "Optical scanning extrinsic Fabry-Perot interferometer for absolute microdisplacement measurement," *Appl. Opt.* 36, 8859-8861 (1997).
16. T.Funabe, N.Tanno, and H.Ito, "Multimode-laser reflectometer with a multichannel wavelength detector and its application," *Appl. Opt.* 36, 8919-8928 (1997).
17. B.S.Lee and T.C.Strand, "Profilometry with a coherence scanning microscope," *Appl. Opt.* 29, 3784-3788 (1990).
18. P.J.Caber, "Interferometric profiler for rough surface," *Appl. Opt.* 32, 3438-3441 (1993).
19. L.Deck and P.de Groot, "High-speed noncontact profiler based on scanning white-light interferometry," *Appl. Opt.* 33, 7334-7338 (1994).
20. O.Sasaki and H.Okazaki, "Sinusoidal phase modulating interferometry for surface profile measurement," *Appl. Opt.* 25, 3137-3140 (1986).
21. K.C.Harvey and C.Myatt, "External-cavity diode laser using a grazing-incidence diffraction grating," *Opt. Lett.* 16, 910-912 (1991).